Comparison of Biomechanical Effects of Different Configurations of Kirschner Wires on the Epiphyseal Plate and Stability in a Salter-Harris Type 2 Distal Femoral Fracture Model

Sermet Inal, MD*
Kadir Gok, PhD†
Arif Gok, PhD‡
Ahmet Murat Pinar, PhD§
Canan Inal, MD||

Background: We sought to investigate the different configurations of Kirschner wires used in distal femur Salter-Harris (SH) type 2 epiphyseal fracture for stabilization after reduction under axial, rotational, and bending forces and to define the biomechanical effects on the epiphyseal plate and the fracture line and decide which was more advantageous.

Methods: The SH type 2 fracture was modeled using design software for four different configurations: cross, cross-parallel, parallel medial, and parallel lateral with two Kirschner wires, and computer-aided numerical analyses of the different configurations after reduction were performed using the finite element method. For each configuration, the mesh process, loading condition (axial, bending, and rotational), boundary conditions, and material models were applied in finite element software, and growth cartilage and von Mises stress values occurring around the Kirschner wire groove were calculated.

Results: In growth cartilage, the stresses were highest in the parallel lateral configuration and lowest in the cross configuration. In Kirschner wires, the stresses were highest in the cross configuration and lowest in the cross-parallel and parallel lateral configurations. In the groove between the growth cartilage and the Kirschner wire interface, the stresses were highest in the parallel lateral configuration and lowest in the cross configuration.

Conclusions: The results showed that the cross configuration is advantageous in fixation. In addition, in the SH type 2 epiphyseal fracture, we believe that the fixation shape should not be applied in the lateral configuration. (J Am Podiatr Med Assoc 109(1): 13-21, 2019)

*Department of Orthopaedic Surgery, School of Medicine, Campus of Evliya Celebi, Kutahya Health Sciences University, Kutahya, Turkey.

†Department of Mechanical and Manufacturing Engineering, Hasan Ferdi, Turgutlu Technology Faculty, Celal Bayar University, Manisa, Turkey.

§Department of Mechanical and Manufacturing Engineering, Technology Faculty, Parmukkale University, Denizli, Turkey.

‡Department of Mechanical Engineering, Technology Faculty, Amasya University, Amasya, Turkey.

||Department of Anesthesiology and Reanimation, Kutahya Education and Research Hospital, Kutahya, Turkey.

Corresponding author: Kadir Gok, PhD, Department of Mechanical and Manufacturing Engineering, Hasan Ferdi Turgutlu Technology Faculty, Celal Bayar University, 45400 Manisa, Turkey. (E-mail: kadir.gok@cbu.edu.tr)

Epiphyseal fracture of the distal femur has high risk, especially in growth interruption and for other complications.[1-4] Among the factors leading to this condition are patient age, type of fracture and degree of dislocation, undulate structure of the physis, and the quality of fracture reduction with the fixation shape.[5-7] Histologic analysis revealed that physeal bar formation was mainly responsible for the angulation at the fracture line and growth complications.[5,8] Generally, for Salter-Harris (SH) type 2 epiphyseal fracture treatment for fixation, straight Kirschner wires passing through the physeal line are used. The size of the Kirschner wire

used during surgery, the sending localization, the number of passes through the physeal line, and the number of Kirschner wires used may increase the injury in the physis. Even for this type of fracture, the treatment objectives are to achieve anatomical reduction and to avoid additional injury to the physis; however, the safest technique has not yet been defined.[5,8-10] Recent studies have shown that an injury to 7% to 9% of the cross-sectional area of the physeal line was sufficient to disrupt growth.[11,12] The aim of the present study was to investigate the different configurations of Kirschner wires used in distal femur SH type 2 epiphyseal fracture for stabilization after reduction under axial, rotational, and bending forces and to define the biomechanical effects on the epiphyseal plate and the fracture line and decide which was more advantageous. Herein, the configurations with the least stress on the epiphyseal plate and the best stability on the fracture line were investigated. Also, the tension passing through the physeal line around the Kirschner wire groove was compared, and the configurations having the highest and lowest tension were investigated. Herein, the highest tension is around the Kirschner wire groove; therefore, it was accepted that bar formation and growth degradation would be increased here, and, thus, from this point of view the best and worst configurations were investigated.

Computer-Aided Three-Dimensional Modeling

The human femoral model was scanned using a three-dimensional (3-D) scanner, and a point cloud was obtained. After that, a 3-D model of the femur was created using point cloud data by the Geomagic Studio 10 program (3D Systems, Rock Hill, South Carolina). This femur model was scaled to take into account the dimensions of a child femur, and an SH type 2 fracture for different configurations was created using a SolidWorks design program (SolidWorks Inc, Waltham, Massachusetts) (Fig. 1). Kirschner wires were used at 2 mm for all of the configurations.

Finite Element Analysis Using a Computer

The computer-aided numerical analysis of stabilization of the different configurations after reduction during fixation was performed using ANSYS Workbench software (ANSYS Inc, Canonsburg, Pennsylvania) based on the finite element method (FEM). The FEM is very important to the development of new surgical techniques. It is also used as a reliable technique for the validation of experimental or analytical results. In addition, several scientists similarly examined the optimal configuration, implant materials, fatigue behavior of implant materials, metal turning, bone drilling, and bone screwing process using the computer-aided finite element analysis (FEA) tool.[13-19] The 3-D CAD models of the different configurations (Fig. 1) were imported into the ANSYS Workbench software to prepare the FEA. Load and boundary conditions and material models were defined in ANSYS Workbench.

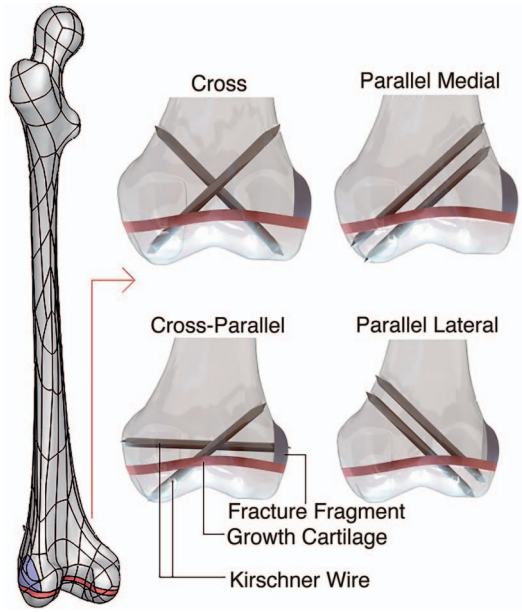


Figure 1. Different configurations for Salter-Harris type 2 fracture.

Loading and Boundary Conditions

After importing the configurations of 3-D models into the ANSYS Workbench software, the mesh process was generated using hex-dominant finite elements for the FEA modeling (Fig. 2). The generated FEA model has 921,966 nodes and 262,219 elements. Although the mesh density for the femur and femur fragment were input as 1 mm, growth cartilage and Kirschner wires were input as 0.25 mm. Axial, bending, and rotational loading were applied to each configuration. A load of 350N in the axial direction was applied to the femoral head, and it was fixed from the epiphyseal plate for axial loading (Fig. 3). Bending forces were applied to the epiphyseal plate in the varus and valgus

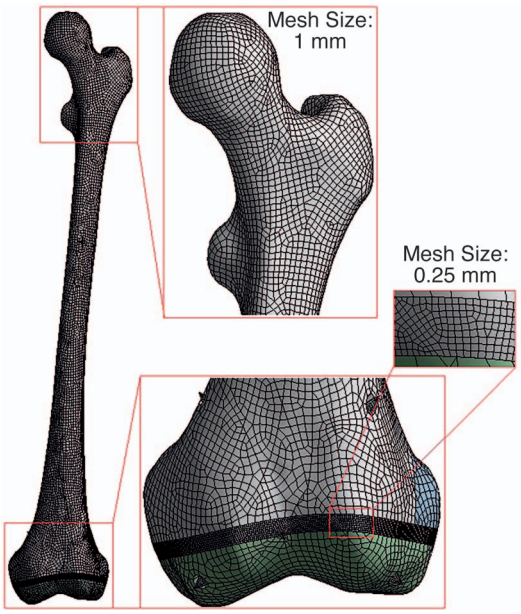


Figure 2. Mesh structure of the configurations.

directions, and the femur was fixed from the metaphysis and the diaphysis (Fig. 3). In addition, bending forces were applied to the epiphyseal plate in the anterior and posterior directions, and the femur was fixed from the metaphysis and the diaphysis. Finally, torsional force was applied to the epiphyseal plate about the z axis in counter clockwise, and the femur was fixed from the metaphysis and the diaphysis. Contact types for bone and bone interactions or Kirschner wire and bone interactions were defined as frictional contact. Friction coefficients were 0.46 for bone–bone interactions and 0.42 for bone–Kirschner wire interactions.[20] The contact type for growth cartilage and Kirschner wires was defined as frictional contact and was 0.04. The contact type for cartilage and bone was defined as bonded.[21] Finally, convergence analysis was conducted (Fig. 4).

Material Model

The mechanical properties of the Kirschner wires (stainless steel), bone, and growth cartilage used in the FEA analyses are given in Table 1. The linear isotropic material model was used for mechanical behaviors of Kirschner wires, bone, and growth cartilage.

Results

After entering the designated loading and boundary conditions, the FEAs were solved. According to the

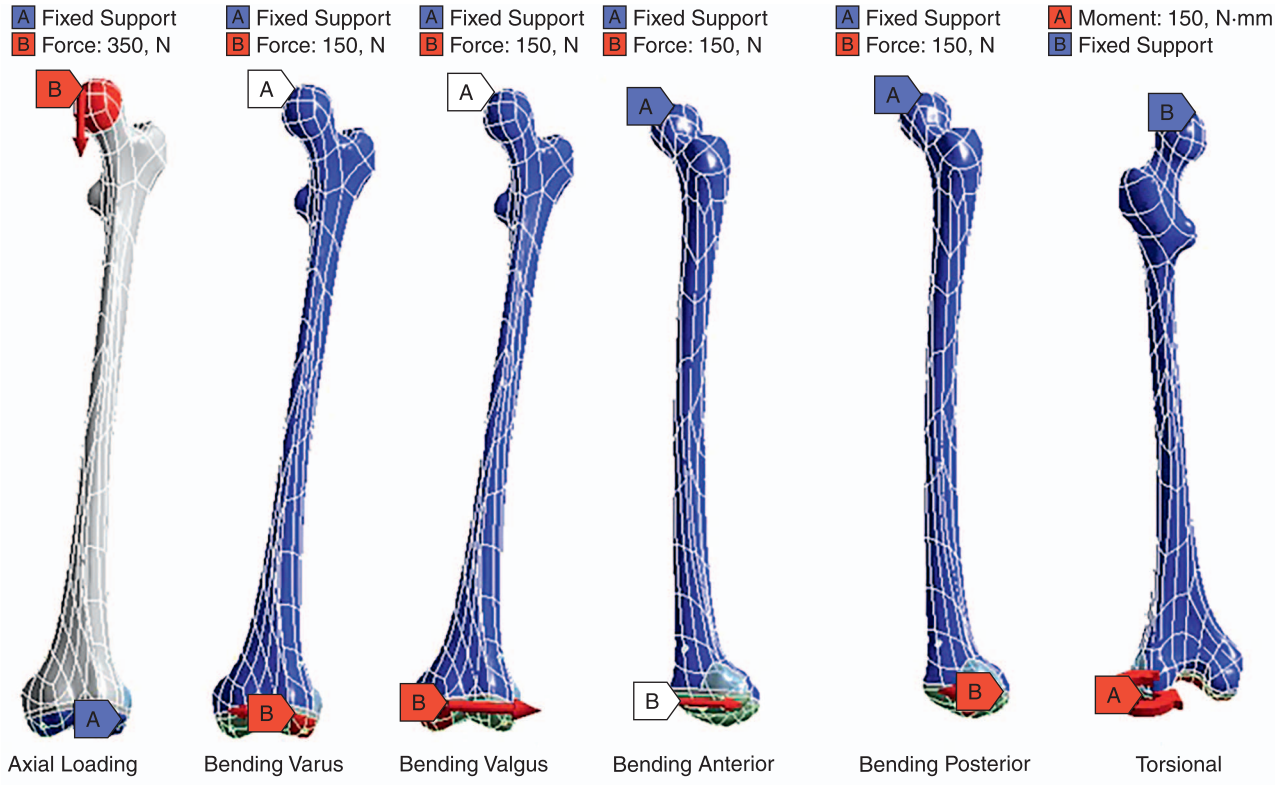


Figure 3. Loading types for different configurations.

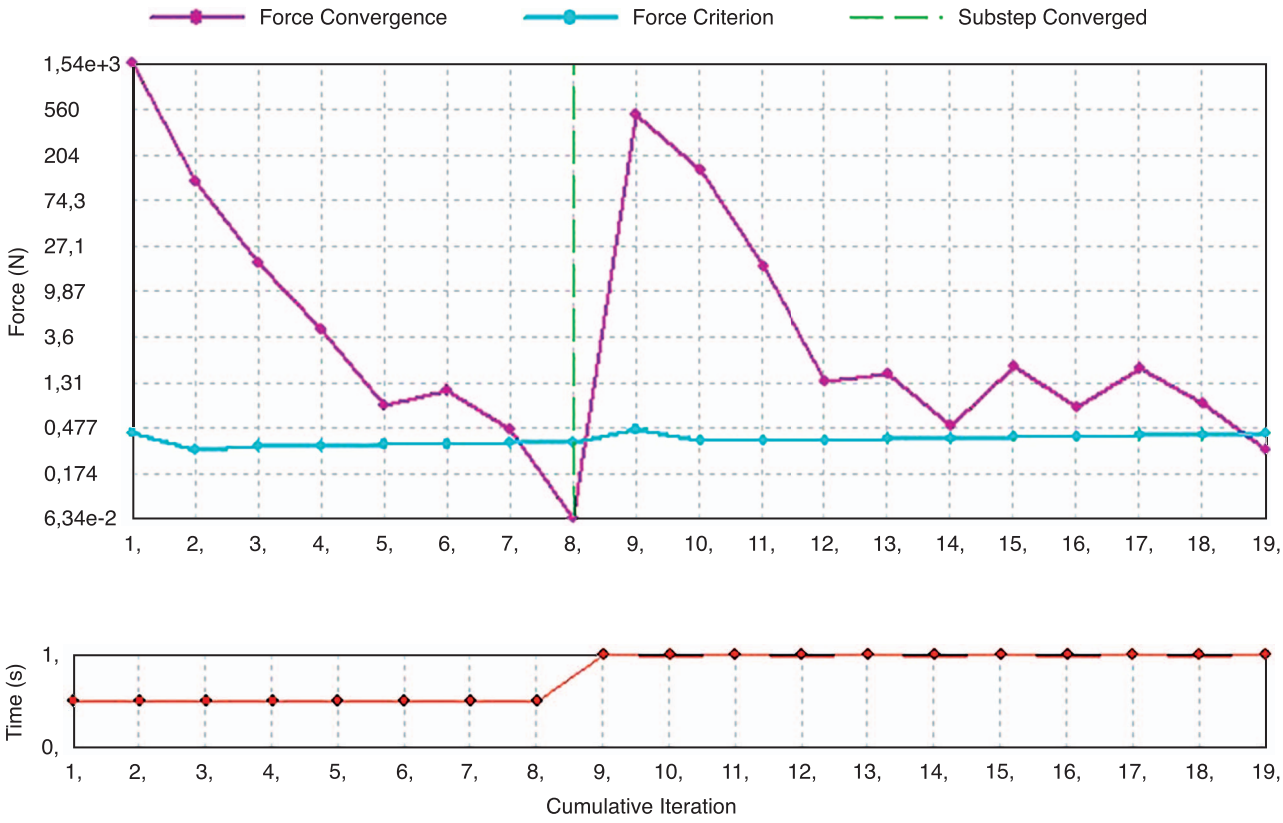


Figure 4. Convergence analysis.

FEA results, stress values in growth cartilage, Kirschner wires, and the groove between the growth cartilage and the Kirschner wire are given in Tables 2 through 4. These stress values were evaluated by the von Mises criteria. In Table 2, under different loads in growth cartilage, the highest stresses were found in the parallel lateral configuration, and the lowest stresses occurred in the cross configuration. In Table 3, the highest stresses were found in the cross configuration, and the lowest stresses occurred in the cross-parallel and parallel lateral configurations. In Table 4, similar to Table 2, in the groove between the growth cartilage and the Kirschner wire interface, the highest stresses were found in the parallel lateral configuration, and the lowest stresses occurred in the cross configuration. Figure 5 shows the stress distributions of different configurations under axial load found in the growth cartilage. Figures 6 through 10 show the stress distributions in the growth cartilage under different loads.

Table 1. Mechanical Properties of Kirschner Wires, Bone, and Growth Cartilage Used in the Finite Element Analyses[22,23]

Parameter	Bone[22]	Kirschner Wires[22]	Growth Cartilage[23]
Density (kg m^{-3})	2,100	7,840	
Young's modulus (MPa)	17,000	210,000	5
Tensile yield strength (MPa)	135	608	
Tensile ultimate strength (MPa)	148	1,000	
Poisson ratio	0.35	0.3	0.46

Discussion

Fixation in the distal epiphysis of the femur in SH type 2 fractures with Kirschner wires can be used in different configurations. In different sources, this fixation has been specified as cross or parallel.[8,9,24-26] However, there is no biomechanical evidence showing which of these configurations with Kirschner wires was more powerful in the stability of a broken line. In addition, in this fixation with Kirschner wires under the stress force loading on the physis, the answer for which the configuration was more or less stress force was completely an open subject. In this study, when we looked into the displacement forces applied to the fracture at the physeal line, the bending forces in the frontal and

Table 2. Stress Values Occurring in the Growth Cartilage

	Loading Type					
Fixation Type	Axial	Bending (Varus)	Bending (Valgus)	Bending (Anterior)	Bending (Posterior)	Torsional
Cross (MPa)	1.96	0.13	0.27	0.32	0.18	0.11
Cross-parallel (MPa)	3.29	0.20	0.46	0.43	0.53	0.13
Parallel lateral (MPa)	4.49	1.75	2.24	1.99	1.98	1.94
Parallel medial (MPa)	3.19	0.14	0.34	0.50	0.57	0.21

Table 3. Stress Values Occurring in the Kirschner Wires

	Loading Type					
Fixation Type	Axial	Bending (Varus)	Bending (Valgus)	Bending (Anterior)	Bending (Posterior)	Torsional
Cross (MPa)	958.58	747.49	443.73	513.67	664.35	569.54
Cross-Parallel (MPa)	824.28	427.69	442.36	495.50	395.19	445.40
Parallel lateral (MPa)	867.61	517.53	411.22	323.14	652.45	462.09
Parallel medial (MPa)	893.65	416.42	546	572.19	489.1	497.17

Table 4. Stress Values Occurring Between the Kirschner Wire and the Growth Cartilage

	Loading Type					
Fixation Type	Axial	Bending (Varus)	Bending (Valgus)	Bending (Anterior)	Bending (Posterior)	Torsional
Cross (MPa)	0.28	0.11	0.21	0.16	0.14	0.11
Cross-parallel (MPa)	0.53	0.08	0.28	0.25	0.21	0.12
Parallel lateral (MPa)	2.21	1.75	2.24	1.99	1.98	1.94
Parallel medial (MPa)	0.86	0.14	0.31	0.28	0.28	0.19

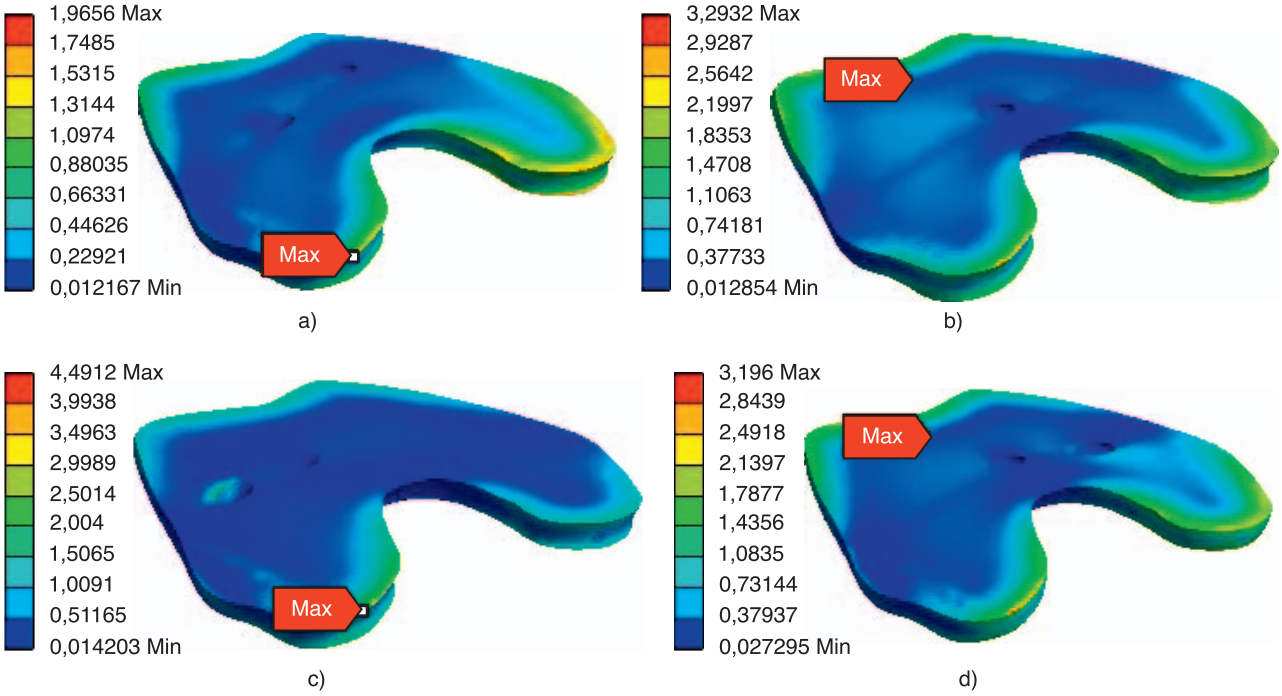


Figure 5. Stress distributions of the different configurations under axial load. A, Cross; B, cross-parallel; C, parallel lateral; and D, parallel medial.

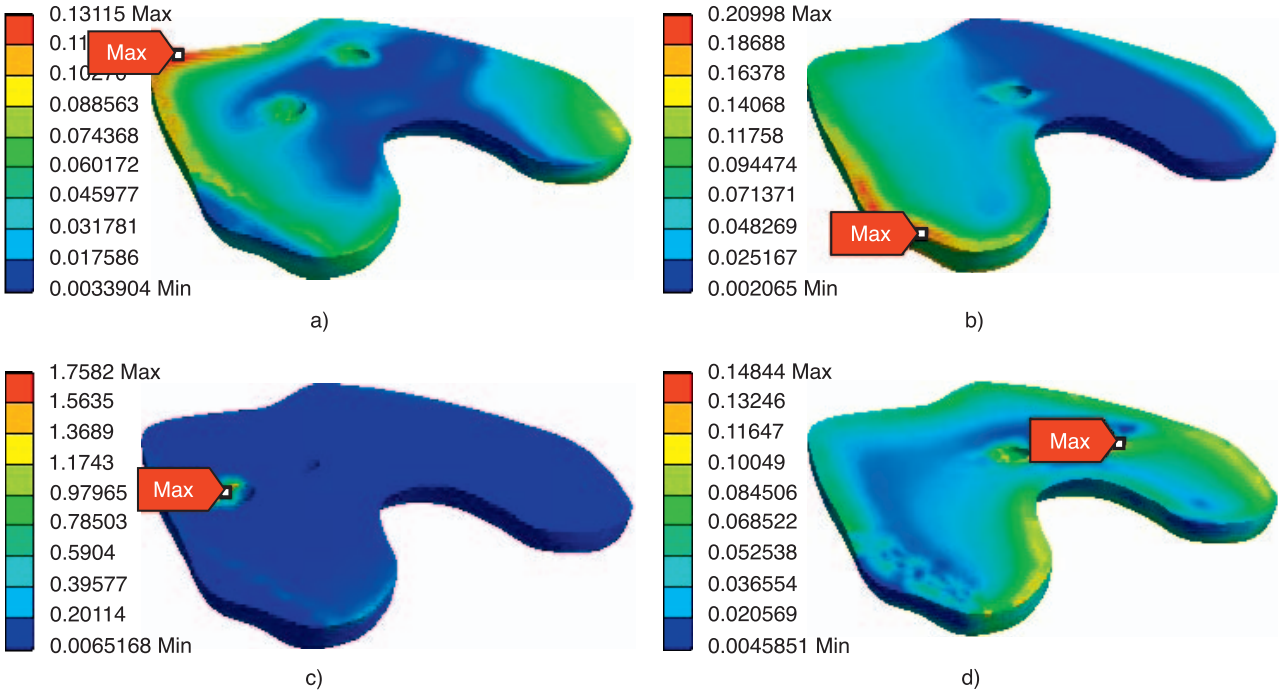


Figure 6. Stress distributions of the different configurations under bending varus load. A, Cross; B, cross-parallel; C, parallel lateral; and D, parallel medial.

sagittal planes (varus-valgus, anterior-posterior displacement), and the torsional forces in the cross configuration, the physeal line was found to have the least stress load. This situation suggested that Kirschner wires took over the stress forces over the fracture line. In fact, the finding of high stresses in Kirschner wires in the cross configuration supported this situation. Under force (axial, bending,

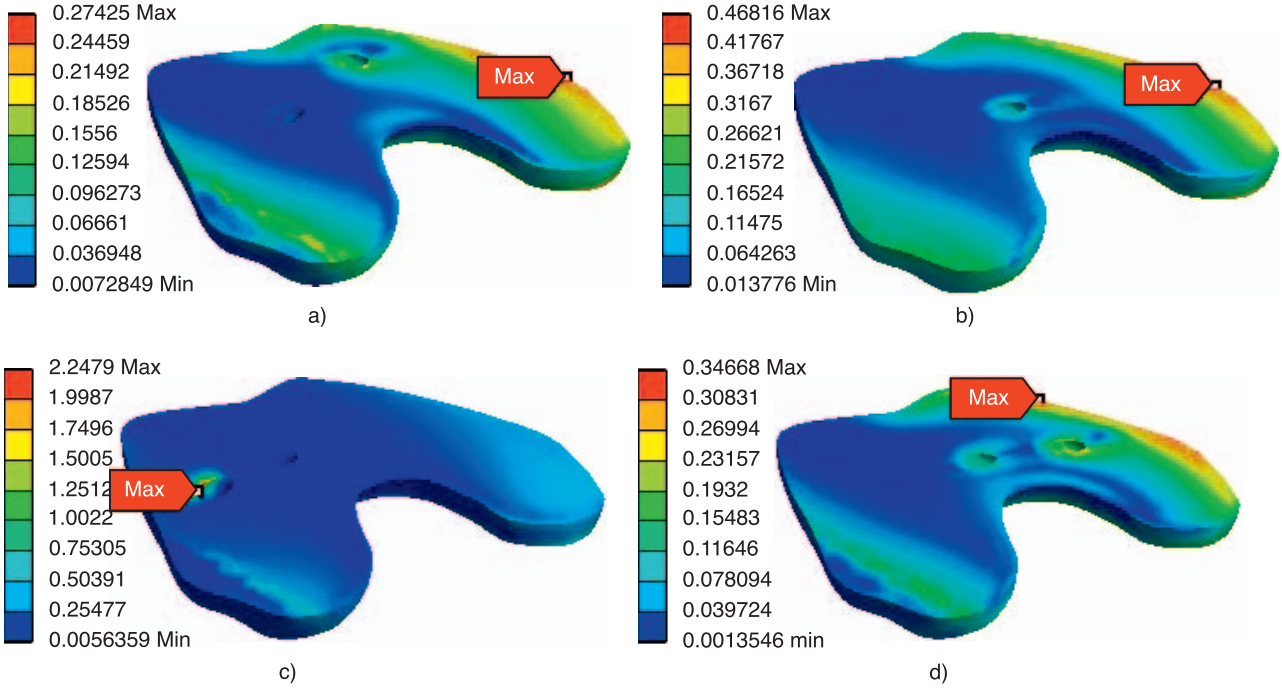


Figure 7. Stress distributions of the different configurations under bending valgus load. A, Cross; B, cross-parallel; C, parallel lateral; and D, parallel medial.

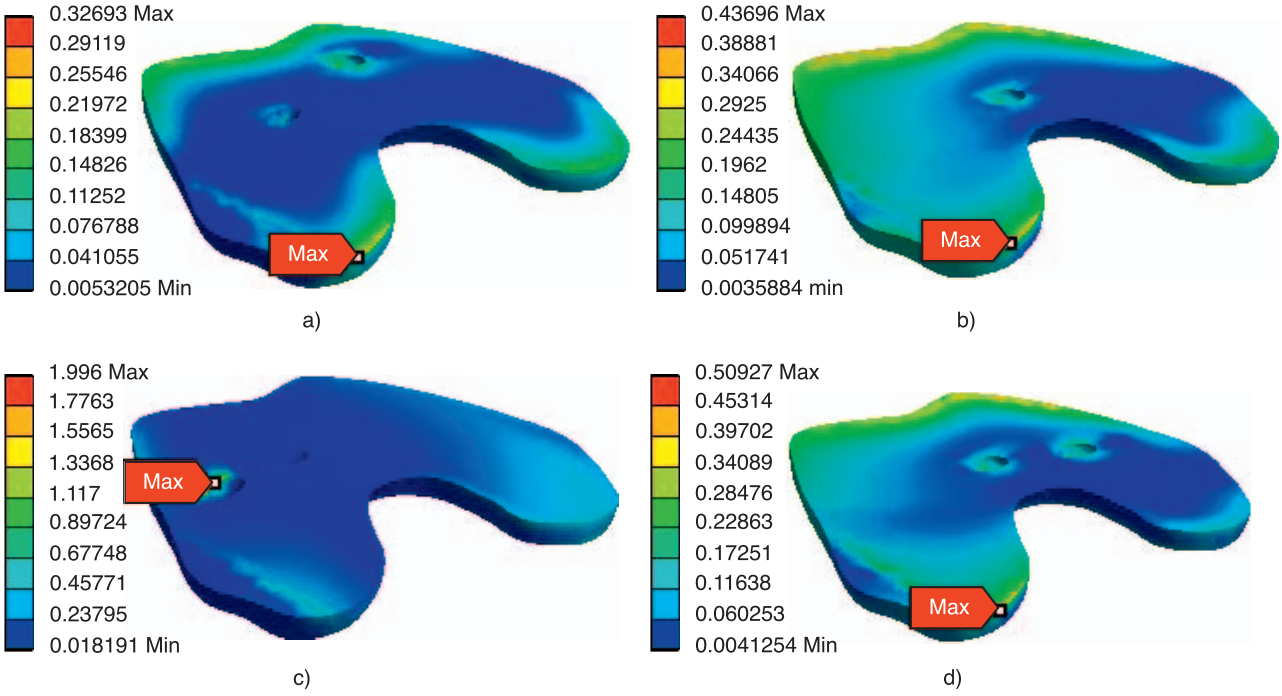


Figure 8. Stress distributions of the different configurations under bending anterior load. A, Cross; B, cross-parallel; C, parallel lateral; and D, parallel medial.

torsional), the more stress on the fracture line, and hence the lowest stability, was found in the lateral configuration, and this was also supported by finding less stress in the Kirschner wires. When we looked at the axial forces in the fracture line in the cross configuration it was determined that the physeal line was least distorted. When we looked at the literature there were no studies about the physis

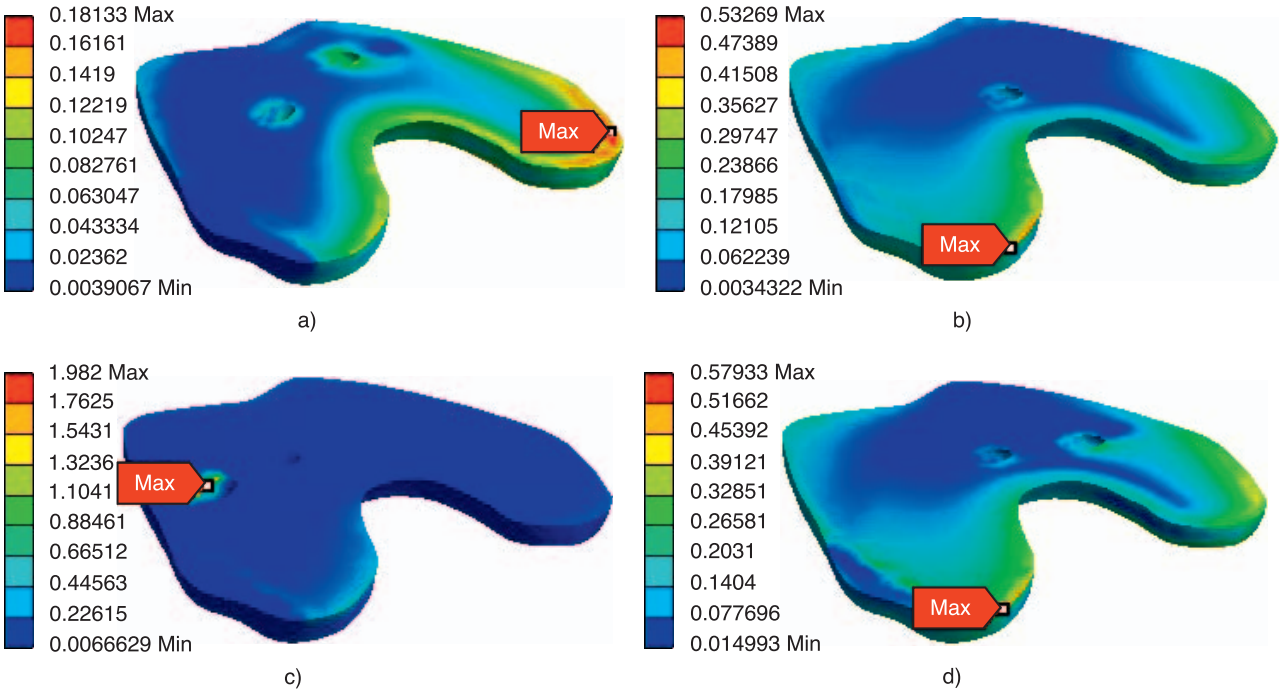


Figure 9. Stress distributions of the different configurations under bending posterior load. A, Cross; B, cross-parallel; C, parallel lateral; and D, parallel medial.

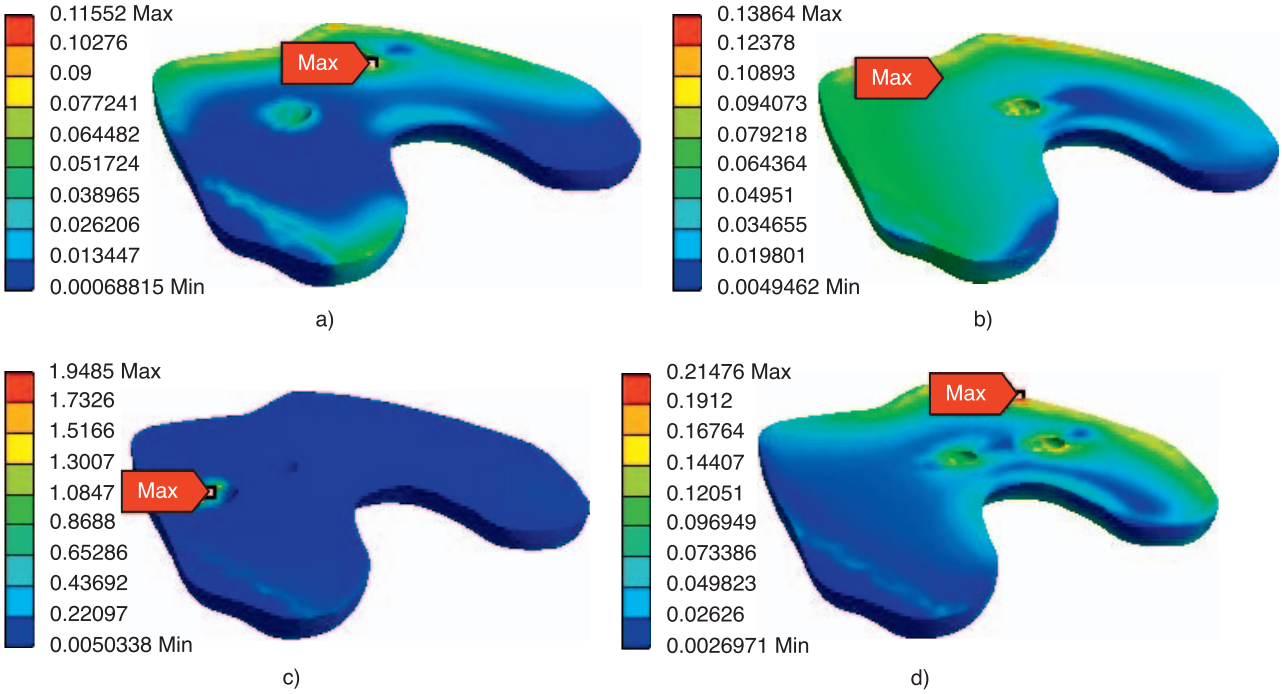


Figure 10. Stress distributions of the different configurations under torsional load. A, Cross; B, cross-parallel; C, parallel lateral; and D, parallel medial.

after fixation and the rate at which it was carrying the stress load. If we think that the worst prognosis of epiphyseal fracture is oppression in the physeal line, we can think that the worst configuration was the most axial stress in the physeal line.[27] In this case, it was seen that the cross configuration had the best stabilization advantages when there were minimal stresses on the physis.

The growth interruption may depend on the type of fracture or on differences in the size of the Kirschner wires used, and physeal bar formation was said to be responsible for this condition.[8,9] After healing of the bone, a bridge is formed in the physis that may be related to the stress load found in the grooves of the Kirschner wires passing from the physis plaques. It is known that Kirschner wires passing through the physis plaque injure the physis. The stress load will be highest in the Kirschner wire groove, and physis injuries will be high and would be responsible for the bar formation at this area. There is no final evidence or biomechanical research that highlights which factors are effective in the formation of iatrogenic epiphysiodesis (bar formation and consequently growth interruption) in this area.

Garrett et al[28] found that SH classification was a prognostic indicator and that smooth Kirschner wires percutaneously passing through the physis were not related to growth retardation. In contrast, in many studies, growth retardation was related to the fixation of this type of fracture.[29] As was mentioned in other studies, we think that one of the markers affecting the outcome was the Kirschner wire configuration, and Kirschner wires passing from the physis would be responsible for the growth retardation. In this study, the results suggest that the cross configuration is advantageous in fixation. In addition, in the SH type 2 epiphyseal fracture, we believe that the necessity of fixation shape should not be applied in the lateral configuration.

Evaluation

In this study, for stabilization of the distal femur after reduction of SH type 2 epiphysis fractures in the use of different configurations of Kirschner wires under axial, rotational, and bending forces, biomechanical behavior on the epiphyseal plate and on the fracture line was examined, and the more advantageous configuration was investigated. According to the FEA results, the cross configuration was found to be most advantageous. Also, in SH type 2 epiphyseal fractures, the parallel lateral

configuration was found to be most disadvantageous.

Financial Disclosure: None reported.
Conflict of Interest: None reported.

References

1. Mann DC, Rajmaira S: Distribution of physeal and nonphyseal fractures in 2, 650 long-bone fractures in children aged 0-16 years. J Pediatr Orthop **10:** 713, 1990.
2. Peterson HA, Madhok R, Benson JT, et al: Physeal fractures: part 1. Epidemiology in Olmsted County, Minnesota, 1979-1988. J Pediatr Orthop **14:** 423, 1994.
3. Basener CJ, Mehlman CT, DiPasquale TG: Growth disturbance after distal femoral growth plate fractures in children: a meta-analysis. J Orthop Trauma **23:** 663, 2009.
4. Eid AM, Hafez MA: Traumatic injuries of the distal femoral physis: retrospective study on 151 cases. Injury **33:** 251, 2002.
5. Dahl WJ, Silva S, Vanderhave KL: Distal femoral physeal fixation: are smooth pins really safe? J Pediatr Orthop **34:** 134, 2014.
6. Liu RW, Armstrong DG, Levine AD, et al: An anatomic study of the distal femoral epiphysis. J Pediatr Orthop **33:** 743, 2013.
7. Lombardo SJ, Harvey JP Jr: Fractures of the distal femoral epiphyses: factors influencing prognosis: a review of thirty-four cases. J Bone Joint Surg Am **59:** 742, 1977.
8. Herring JA, ed: "Lower Extremity Injuries," *Tachdjian's Pediatric Orthopaedics*, p 2327, WB Saunders Co, Philadelphia, 2002.
9. Zionts LE: "Fractures and Dislocations About the Knee," in *Skeletal Trauma in Children*, p 443, WB Saunders Co, Philadelphia, 2003.
10. Arkader A, Warner WC Jr, Horn BD, et al: Predicting the outcome of physeal fractures of the distal femur. J Pediatr Orthop **27:** 703, 2007.
11. Garcés GL, Mugica-Garay I, López-González Coviella N, et al: Growth-plate modifications after drilling. J Pediatr Orthop **14:** 225, 1994.
12. Janarv P-M, Wikström B, Hirsch G: The influence of transphyseal drilling and tendon grafting on bone growth: an experimental study in the rabbit. J Pediatr Orthop **18:** 149, 1998.
13. Gok K, Inal S, Gok A, et al: Biomechanical effects of three different configurations in Salter Harris type 3 distal femoral epiphyseal fractures. J Braz Soc Mechanical Sci Eng **39:** 1069, 2017.
14. Gok K: Development of three-dimensional finite element model to calculate the turning processing parameters in turning operations. Measurement **75:** 57, 2015.
15. Inal S, Taspinar F, Gulbandilar E, et al: Comparison of the biomechanical effects of pertrochanteric fixator and dynamic hip screw on an intertrochanteric femoral fracture using the finite element method. Int J Med Robotics Computer Assisted Surg **11:** 95, 2015.
16. Erdem M, Gok K, Gokce B, et al: Numerical analysis of temperature, screwing moment and thrust force using finite element method in bone screwing process. J Mechanics Med Biol **17:** 1750016, 2017.
17. Gok A, Inal S, Taspinar F, et al: Fatigue behaviors of different materials for schanz screws in femoral fracture model using finite element analysis. Optoelectron Adv Mat **8:** 576, 2014.
18. Afsar E, Taspinar F, Calik BB, et al: Use of the finite element analysis to determine stresses in the knee joints of osteoarthritis patients with different Q angles. J Braz Soc Mechanical Sci Eng **39:** 1061, 2017.
19. Gok K, Taspinar F, Inal S, et al: Importance of sidebar-bone spacing during the application of pertrochanteric fixator on femoral intertrochanteric fracture model; comparison of the biomechanical effects using finite element method. Biomed Eng **27:** 1550030, 2015.
20. Goffin JM, Pankaj P, Simpson AH: The importance of lag screw position for the stabilization of trochanteric fractures with a sliding hip screw: a subject-specific finite element study. J Orthop Res **31:** 596, 2013.
21. Atmaca H, Kesemenli C, Memişoğlu K, et al: Changes in the loading of tibial articular cartilage following medial meniscectomy: a finite element analysis study. Knee Surg Sports Traumatol Arthrosc **21:** 2667, 2013.
22. Yuan-Kun T, Yau-Chia L, Wen-Jen Y, et al: Temperature rise simulation during a Kirschner pin drilling in bone. Paper presented at: the 3rd International Conference on Bioinformatics and Biomedical Engineering, Beijing, June 11-13, 2009.
23. Peña E, Calvo B, Martínez MA, et al: Finite element analysis of the effect of meniscal tears and meniscectomies on human knee biomechanics. Clin Biomech **20:** 498, 2005.
24. Agus H, Kalenderer O, Kayali C. "Çocuklarda Alt Ekstremite Kiriklari" in Çocuk Ortopedisi, edited by E Çullu, p 67-84, Bayçinar Tıbbi Yayıncılık, İstanbul, 2012.
25. Wheeless CR III: Wheeless' textbook of orthopaedics. Available at: http://www.wheelessonline.com/ortho/distal_femoral_physeal_fractures. Published 2014. Accessed December 18, 2017.
26. Müller ME, Allgöwer M, Schneider R, et al: "Fractures in Children," in *Manual of Internal Fixation*, p 689, Springer-Verlag, New York, 1995.
27. Seyhan F, Goksan SB: "Çocuk Kırıkları," in Ortopedik Travmatoloji, edited by Alturfan AK, p 89-101, Nobel Tıp Kitabevleri, İstanbul, 2002.
28. Garrett BR, Hoffman EB, Carrara H: The effect of percutaneous pin fixation in the treatment of distal femoral physeal fractures. J Bone Joint Surg Br **93:** 689, 2011.
29. Wall EJ, May MM: Growth plate fractures of the distal femur. J Pediatr Orthop **32:** S40, 2012.